PHYSICAL REVIEW B VOLUME 32, NUMBER 6 15 SEPTEMBER 1985

Equation of state and properties of lithium

J. C. Boettger
Theoretical Division, Los Alamos National Laboratory, University of California, Los Alamos, New Mexico 87545

S. B. Trickey
Quantum Theory Project, Department of Physics and Department of Chemistry, University of Florida, Gainesville, Florida 32611

(Received 2 April 1985)

The equation of state and one-electron properties of fcc and bcc Li are calculated for cell volumes between 0.175 and 3.0 times the experimental zero-pressure volume with use of the linear-combination-of-Gaussian-type-orbitals technique. These calculations utilize two distinct local-density-approximation (LDA) models. The fcc structure is found to be more stable for all volumes considered and for both LDA models, contrary to a recent prediction of bcc stability at high pressures. The bulk properties exhibit LDA-model dependencies similar to those recently noted in Fe, i.e., the best accord with experiment is achieved with the simple Kohn-Sham-Gaspar model. This somewhat surprising outcome holds not only at equilibrium but for pressures up to 250 kbar. The high-pressure band structure of Li is also presented for the first time. That band structure exhibits rather interesting modifications compared to the zero-pressure band structure.

I. INTRODUCTION

The cohesive properties of lithium were first investigated by Wigner and Seitz[1] as part of their pioneering work on metals during the mid-1930's. Since that time there have been numerous theoretical studies of Li, including one-electron properties,[2,3] zero-pressure bulk properties,[2,4–15] equation of state (EOS),[16–19] and crystallographic phase stability.[8,18–21] (For an extensive list of theoretical work prior to 1974 see Ref. 2.) In spite of that activity, theoretical understanding of this simple alkali metal remains deficient in three respects. (1) Because radically different techniques have been used for calculations of different physical properties, it is impossible to construct a consistent theoretical picture of Li including both one-electron and bulk properties over a wide range of pressures. (2) In spite of experimental evidence[22] which indicates that at low pressures and temperatures Li is in a close-packed structure (hcp or fcc), all of the one-electron results published to date have been for the bcc structure observed at room temperature. (3) The only two theoretical investigations of the phase stability of Li as a function of increasing pressure[18,19] are in fundamental disagreement.

The third point is particularly urgent. Using model potentials, Young and Ross[18] predicted two transitions below 1 Mbar on the 0-K isotherm: hcp-fcc at about 4 kbar and fcc-bcc at about 86 kbar. On the other hand, a very recent calculation by Skriver[19] using the linear-muffin-tin-orbitals (LMTO) method indicates only one transition, hcp-fcc at about 210 kbar. It is particularly important that the existence or nonexistence of an fcc-bcc transition should be clarified since the predicted pressure lies well within the reach of current diamond anvil techniques.[23]

We have addressed the problems just described by performing high-precision calculations of the 0-K isotherms for fcc and bcc Li (the techniques used here are currently restricted to cubic symmetries). These calculations were performed within the local density approximation (LDA) to density-functional theory.[24,25] In recent years, total energy calculations based on the LDA have been applied with considerable success to such sensitive problems as binding in rare-gas crystals[26–28] and the phase stability of both crystalline solids[19,29–35] and thin films.[36,37] To achieve high precision and therefore a faithful representation of the physical content of a specified LDA model, without invoking additional major approximations, we have employed the linear-combinations-of-Gaussian-type-orbitals (LCGTO) technique.[26,29] This approach has several distinct advantages over more commonly used methods for a study of this sort. Unlike pseudopotential methods,[15–18,32,33,35] the LCGTO technique is an all-electron method. It is also independent of such potential and/or charge shape approximations as the muffin-tin approximation used in augmented-plane-wave[5,7] (APW) and Korringa-Kohn-Rostoker[10] (KKR) methods or the atomic-sphere approximation[38] (ASA) frequently used in the LMTO method.[19,34,35,38] Freedom from the above-mentioned constraints may be of particular importance for systems such as Li for which the structural energy differences are believed to be quite small.[8,15,18–21]

In the following section, we briefly discuss some of the details of our calculations and provide a conservative estimate of their overall numerical precision. In Sec. III, LCGTO results are presented for the 0-K isotherms of fcc and bcc Li, including both zero-pressure cohesive properties and high-pressure phase stability. To study any possible dependencies of the results on the choice of LDA model, we have obtained the 0-K isotherm for both the Kohn-Sham-Gaspar (KSG) model,[25] i.e., $X\alpha$ with $\alpha=\frac{2}{3}$, and the von Barth—Hedin (VBH) model[39] using the parameters suggested by Rajagopal, Singhal, and Kimball (RSK).[40] We find that Li exhibits LDA model dependencies which resemble those recently found in Fe by Jansen *et al.*[41] In Sec. IV, we briefly examine the one-electron properties of Li at low and high pressures using the RSK potential. Conclusions are presented in Sec. V.

II. METHODOLOGICAL DETAILS

The procedures used here to achieve reliable crystalline total energy calculations are an extensive refinement[26] of ideas introduced by Callaway *et al.*[13] based on the LCGTO scheme presented by Wang and Callaway.[42] (The full technical details are presented in Refs. 26, 42, and 43.) The refinements introduced in Ref. 26 were specific to $X\alpha$ type LDA models. To extend the total energy calculations to general LDA models, one must replace Eq. (11) of Ref. 26 with

$$E_{\mathrm{xc}}=N\Omega\sum_{\mathbf{k}}\{[V^0_{\mathrm{xc}}(\mathbf{K})-W^0_{\mathrm{xc}}(\mathbf{K})]\rho^0(\mathbf{K})+V^0_{\mathrm{xc}}(\mathbf{K})\delta\rho(\mathbf{K})+\tfrac{1}{2}\delta V_{\mathrm{xc}}(\mathbf{K})\delta\rho(\mathbf{K})\}\ . \qquad (1)$$

(Throughout, we shall employ the notation and terminology of Ref. 26.) The virial pressure may also be generalized[44] by replacing Eq. (13) of Ref. 26 with

$$P=(1.470\,99\times10^5)\times\left[\frac{E+T}{3N\Omega}+\tfrac{1}{3}\sum_{\mathbf{K}}[4W_{\mathrm{xc}}(\mathbf{K})-V_{\mathrm{xc}}(\mathbf{K})]\rho(\mathbf{K})\right]\ . \qquad (2)$$

Note that other expressions which are analytically equivalent to Eqs. (1) and (2) are in practice numerically unstable.[26]

In any LCGTO methodology, the choice of the basis set is crucial. In this investigation we have used the $10s\,6p\,3d$ basis given in Ref. 26 for all cell volumes greater than 120.0 a.u. This basis set is very nearly saturated[26] and should not have any significant effect on our final results. For smaller volumes, the basis set was scaled to avoid near-linear dependencies. The most diffuse Gaussian was scaled by requiring that its value on the nearest-neighbor site should remain the same as it was for a volume of 131.072 a.u. (roughly the calculated equilibrium volume for the RSK model). This corresponds to a $(1/a)^2$ scaling of the smallest exponent. The remaining exponents were scaled by requiring that no exponent could be less than twice as large as the next smaller exponent. Diagonalization of the overlap matrices at high-symmetry points in the irreducible part of the Brillouin zone (BZ) shows no indication of linear dependence at compressed volumes.

In the Wang-Callaway formulation of the LCGTO method, Fourier-transform techniques are used extensively and the quality of the results is dependent therefore on various truncation points in reciprocal space. The impact of these truncations on structural energy differences was minimized by choosing analogous truncation points in both structures. The total number of Fourier coefficients considered was truncated at $K_M^2=4000$ (6300) for the bcc (fcc) structure. These values correspond to 12 014 or 12 152 independent Fourier coefficients, respectively. In the self-consistent cycle 99 (100) independent Fourier coefficients were allowed to vary for the bcc (fcc) structure. Based on prior experience with Li,[26] we estimate that these truncations may produce an error of 0.3 mRy in the total energy for either structure. The impact on the structural energy differences should be much less.

During the self-consistent cycle, the charge density for the bcc (fcc) structure was constructed by sampling 55 (20) **k** points in the irreducible part of the BZ. In earlier work on fcc Al,[45] it was found that increasing the number of points sampled in the self-consistent cycle from 20 to 89 changed the final energy by less than 0.01 mRy. We expect Li to be a much better case than Al. Using a dynamical convergence accelerator,[43] self-consistency (defined by an iterative shift in total energy of less than 0.01 mRy) was generally achieved within seven iterations. The one-electron eigenvalues were then recalculated at 506 (505) **k** points in the irreducible part of the BZ for the bcc (fcc) structure. Based on convergence studies, we estimate that this density of **k** points ensures that the sum of the eigenvalues (used in the total energy calculation[26]) is converged to within 0.5 mRy for either structure and that the difference between the sums for the fcc and bcc structures is stable to within 0.05 mRy.

In the current LCGTO technique, the most difficult approximation to control is the linearized density shift expansion for the exchange-correlation potential,[26] which in turn is the source of the second-order expansion for the exchange-correlation energy in Eq. (1). The quality of this approximation was monitored by comparing the sizes of the first- and second-order terms in Eq. (1) for every calculation. Taking this approximation and the approximations discussed above into account, we estimate that for volumes less than 150.0 a.u. the binding energies obtained are stable to within 1 mRy and the structural energy differences at equal volumes are stable to within 0.1 mRy. The assessment of imprecision for expanded lattices is more intricate; see below.

III. BULK PROPERTIES AT 0 K

The total energy and pressure of Li were calculated for nine volumes in each crystal structure (fcc and bcc) using both the KSG and RSK models. The raw results are in Tables I and II. For each LDA model, four of the volumes were chosen to lie close to the apparent energy minimum to allow a very precise determination of zero-pressure properties. The remaining volumes used for each structure were selected to sample the EOS at reasonably uniformly spaced volumes ranging from near the experimental zero-pressure volume of 142.44 a.u. (Ref. 46) to about 0.175 of that volume.

A. Qualitative analysis

Table III compares the structural energy differences obtained from the KSG model with those from the RSK model at six volumes. Clearly, the fcc structure is lower in energy for the entire range of volumes considered for both models, in qualitative agreement with Skriver.[19] In fact, the energy of the fcc structure progressively becomes lower relative to the bcc structure as the pressure is increased. This finding is in direct conflict with the results obtained by Young and Ross,[18] which indicated that the

TABLE I. The calculated total energies per atom (Ry) and pressures (kbar) for fcc and bcc Li using the RSK potential as a function of cell volume (a.u.).

V	E(fcc)	P(fcc)	E(bcc)	P(bcc)
428.686	−14.836 796	−36.4	−14.833 679	−32.9
312.416	−14.878 482	−44.4	−14.877 950	−42.4
212.443	−14.907 733	−44.2	−14.907 673	−43.3
162.456	−14.919 735	−33.3	−14.919 280	−32.5
143.748	−14.922 815	−22.7	−14.922 152	−21.8
131.072	−14.923 955	−11.1	−14.923 148	−10.1
128.024	−14.924 072	−7.6	−14.923 229	−6.5
125.023	−14.924 113	−3.8	−14.923 235	−2.6
122.070	−14.924 075	0.4	−14.923 164	1.6
99.973	−14.920 104	50.4	−14.919 013	52.0
74.980	−14.901 130	193.9	−14.899 613	196.7
49.987	−14.835 601	691.6	−14.833 153	698.6
24.993	−14.542 938	3741.0	−14.536 896	3736.0

bcc structure was more stable for pressures above 86 kbar. Young and Ross, however, also found that for any temperature and pressure at which the fcc structure is stable, a transition to the bcc structure could be induced by increasing the pressure. That result is in disagreement with the experimental 300-K isotherm published by Olinger and Shaner[47] which shows that the bcc structure is stable below 69 kbar and the fcc structure is stable at higher pressures. This disagreement with experiment (at 300 K) is so fundamental that it renders the entire phase diagram (including the 0-K isotherm) presented in Ref. 18 suspect.

Although we found no fcc-bcc transition at compressed volumes, there is also the question of how Li would behave in the expanded lattice limit. To explore this regime, we performed calculations at four expanded volumes using the RSK model (see Table I). For these volumes the density shift expansions, Eq. (1), becomes progressively worse and the results are questionable. Nevertheless, all of the calculations place the fcc structure lower in energy than the bcc structure and it at least appears there are no transitions to the bcc structure for cell volumes ranging from 0.175 to 3.0 times the experimental zero-pressure volume.

In addition to possible crystallographic phase transitions, we would anticipate that in the expanded lattice limit there should be a Mott transition[48] to an insulating, spin-polarized state since the free atom is spin polarized. This possibility was explored by Callaway, Zou, and Bagayoko[14] (CZB) using their original LCGTO techniques (i.e., without the refinements of Ref. 26). They predicted that bcc Li would have a partially spin-polarized metallic ground state for lattice constants between 10.7 and 11.3 a.u., while the ground state for larger lattice constants is fully spin-polarized and insulating. Furthermore, they also found a shallow energy minimum at about 13.0 a.u.

To test the expanded lattice results obtained by CZB, using the more refined techniques, we performed both paramagnetic and spin-polarized calculations (with the initial spin density saturated) for the bcc phase at the reported minimum, 13.0 a.u. The spin polarization of the ferromagnetic state persisted in the self-consistent calculation and produced a lower energy than the paramagnetic state. Although this result is in qualitative agreement with CZB, there is a severe difficulty. The density shift expansion for the exchange-correlation energy, Eq. (1), was clearly unstable. For the majority spin, the second-order term was larger than the first-order term, with all three terms being negative. For the minority spin the first- and second-order terms were positive and negative, respectively, and both were on the order of 100 mRy. This suggests that the expansion for the majority spin is a diverging sum, while the expansion for the minority spin at best is only conditionally convergent. We were thus unable to determine the point at which the Mott transition occurs in Li using the current approximations.

TABLE II. The calculated total energies per atom (Ry) and pressures (kbar) for fcc and bcc Li using the KSG potential as a function of cell volume (a.u.).

V	E(fcc)	P(fcc)	E(bcc)	P(bcc)
147.040	−14.475 873	−9.3	−14.475 472	−8.4
143.748	−14.475 966	−6.5	−14.475 527	−5.6
140.506	−14.475 977	−3.5	−14.475 481	−2.6
137.313	−14.475 885	−0.3	−14.475 390	0.6
131.072	−14.475 586	6.9	−14.474 988	8.0
99.973	−14.467 039	75.7	−14.466 179	77.3
74.980	−14.442 849	230.0	−14.441 514	232.8
49.987	−14.369 403	751.2	−14.367 194	758.1
24.993	−14.061 886	3850.8	−14.056 108	3844.9

TABLE III. The structural energy difference $E(\text{bcc}) - E(\text{fcc})$ (mRy) for Li as a function of cell volume (a.u.).

V	ΔE(RSK)	ΔE(KSG)
143.748	0.66	0.44
131.072	0.81	0.60
99.973	1.09	0.86
74.980	1.52	1.34
49.987	2.45	2.21
24.993	6.04	5.78

B. Theoretical zero-pressure results

To extract quantitative results from the raw data in Tables I and II, we must fit that data to some analytical form for the EOS. For each LDA model and crystal structure we have determined the bulk properties at zero pressure by fitting the energies at the four volumes nearest to the energy minimum with the Murnaghan equation.[49] (The quality of the fit achieved here and below was such that the more elaborate fitting scheme used in Ref. 29 was deemed unnecessary.) Since the E versus V version of the Murnaghan equation has four free parameters, we are able to extract the minimum energy, the zero-pressure lattice constant, and the bulk modulus from an exact fit. To obtain the binding energy we used the energy of the spin-polarized atom computed with the enriched basis set described in Ref. 26. (In that work the paramagnetic atom was used as reference.) The atomic energies for the KSG and RSK models are -14.386567 Ry and -14.786866 Ry, respectively. The results for the equilibrium properties are given in Table IV together with other LDA results[6,7,10] and experimental values.[46,50] For purposes of comparison with Ref. 10, we also performed a single calculation for bcc Li using the Hedin-Lundqvist (HL) parameters[51] at a lattice constant of 6.40 a.u. Based on the virial pressure at that single point, we are able to estimate the equilibrium lattice constant as well as the binding energy (see Table IV).

Comparison of the bcc results obtained in this study using the KSG and HL models with those obtained in previous calculations using the same models,[7,10] shows that the current non-muffin-tin results for the lattice constant are contracted relative to the earlier muffin-tin results. This finding is consistent with recent work on Al (Ref. 29) using the KSG model and may be viewed as a relaxation of the crystal when the muffin-tin constraint is removed. For both the KSG and the HL models, the calculated LCGTO binding energies are in excellent agreement with the previous results. For the bulk modulus, the present values are larger than those obtained using muffin-tin methods (assuming that the RSK and HL bulk moduli differ negligibly). This discrepancy is due in part to the lattice contraction discussed above, for as the volume is decreased the bulk modulus increases.

Comparison of the present RSK results for bcc Li with those of CZB warrants careful analysis. Compared to the present results, CZB found a larger lattice constant, a smaller binding energy, and a smaller bulk modulus. In each instance, the value found by CZB lies closer to experiment. However, the algorithms used here are numerically more stable than those used by CZB.[26] Also, the basis set used here is richer than that used by CZB and most of the precision-determining input parameters for these calculations (e.g., the truncation points in reciprocal space and the BZ scan) are less restrictive. Therefore the present calculation should represent the physical content of the LDA models in use more faithfully than the calculations by CZB. The better agreement with experiment in Ref. 14 is probably due to a fortuitous cancellation of LDA and algorithmic deficiencies.

For the bcc structure it is possible to compare the theoretical results with experiment.[46,50] Such a comparison reveals some interesting dependencies on the choice of the LDA model. The simplest possible LDA model (KSG) produces significantly better results for the structural properties (the lattice constant and bulk modulus) than do the more sophisticated VBH-type schemes (RSK) and HL). In fact, the KSG lattice-

TABLE IV. The lattice constant (a_0), static lattice binding energy (E_b), and bulk modulus (B) of Li found in this study for the bcc and fcc structures compared to previous calculations and to experiment.

Model	Method		Structure	a_0 (a.u.)	E_b (mRy)	B (Mbar)
KSG	LCGTO	Present	bcc	6.59	-88.9	0.147
KSG	APW	Ref. 7	bcc	6.64	-86.7^{a}	0.115
HL	LCGTO	Present	bcc	6.35^{b}	-124	
HL	KKR	Ref. 10	bcc	6.42	-124	0.148
RSK	LCGTO	Present	bcc	6.32	-136.4	0.158
RSK	LCGTO	Ref. 14	bcc	6.52	-127	0.138
Liberman	KKR	Ref. 6	bcc	6.46	-127	0.131
expt.			bcc	6.58^{c}	-122^{d}	0.126^{c}
KSG	LCGTO	Present	fcc	8.28	-89.4	0.187
RSK	LCGTO	Present	fcc	7.94	-137.3	0.168

[a] The energy reported in Ref. 7 was calculated relative to the paramagnetic atom. We have adjusted that energy by the appropriate spin polarization energy, 37.1 mRy.

[b] Estimated based on one calculation at 6.40 a.u.

[c] Reference 46.

[d] Reference 50.

constant prediction agrees with experiment to within the numerical precision of the theoretical result (0.01 a.u.), while the VBH-type models give a significantly contracted lattice constant. This result is consistent with those of Jansen *et al.*[41] for Fe. They found that for three successively more refined LDA models the calculated equilibrium lattice constant became successively more contracted. Jansen *et al.*[41] argued that the problem lies with the neglect of nonlocal contributions to the exchange-correlation potential. Although their explanation is quite reasonable, it does not account for the good theoretical lattice constants obtained using the KSG model for both Li and Fe. In spite of the good structural properties obtained with the KSG model, that model also produces a 27% underbinding compared to the experimental estimate of the bcc binding,[50] while the HL model is in nearly perfect agreement.

In Table V, we compare the zero-pressure structural energy differences found here with prior results.[19–21] It is interesting that the differences found in the other three calculations are significantly smaller than the LCGTO values. This trend is probably due to the lack of overall self-consistency in the earlier results. The two model-potential calculations[20,21] were constrained by both the frozen-core approximation and the form of the model potential. In the LMTO calculation[19] not only were the cores frozen but the total potential was only calculated self-consistently for one reference structure (the structural energy difference was found with the so-called force theorem[52]). Presumably the error generated in the three earlier calculations by not allowing the system to relax fully accounts for the discrepancy. The LMTO underestimate of the structural energy difference also is consistent with earlier findings for Al.[29]

C. The equation of state

To study the EOS for Li, we fitted the fcc results in Tables I and II to the E versus V version of the Murnaghan equation for the RSK and KSG models. (We only used the eight smaller volumes for the RSK model.) The calculated and fitted pressures are compared in Table VI. Also included in Table VI are the parameters needed to construct the entire P versus V curve in the form

$$P=(B/\gamma)[(V_0/V)^{\gamma}-1] . \tag{3}$$

(The equilibrium volumes and bulk moduli given in Table VI differ from those in Table IV because fitting over a large pressure range has reduced somewhat the quality of the fit in the equilibrium region.) For both models, the fitted pressures deviate by no more than 25 kbar from the calculated pressures up to 700 kbar. For pressures between 700 kbar and nearly 4 Mbar the deviation increases to an overestimate of about 300 kbar (a 7.5% error). The deterioration of the fit with increasing pressure is not surprising since the Murnaghan equation was originally intended as a tool for extrapolating low-pressure experimental data to moderate pressures.

TABLE V. The zero-pressure structural energy difference, $E(\text{bcc})-E(\text{fcc})$ (mRy) for Li found in this study using the KSG and RSK models compared to previous calculations.

Model	Calculation	Ref.	ΔE
KSG	LCGTO	Present	0.47
RSK	LCGTO	Present	0.87
VBH	LMTO	Ref. 19	0.16
Model potential		Ref. 20	−0.02
Model potential		Ref. 21	0.10

TABLE VI. The calculated virial pressures (P_v) compared with the pressures obtained by fitting the energies to the Murnaghan equation (P_f) for the KSG and RSK models. Also the characteristic parameters (V_0, B, and γ) required to specify the entire fitted EOS.

	KSG		RSK	
V	P_v (kbar)	P_f (kbar)	P_v (kbar)	P_f (kbar)
147.0411	−9.3	−10.3		
143.7491	−6.5	−6.9		
140.5066	−3.5	−3.2		
137.3132	−0.3	0.6		
131.0723	6.9	9.1	−11.1	−12.8
128.0240			−7.6	−8.5
125.0234			−3.8	−3.9
122.0700			0.4	1.0
99.9732	75.7	82.5	50.4	55.4
74.9799	230.0	234.8	193.9	198.6
49.9866	751.2	735.7	691.6	676.7
24.9933	3850.8	4159.5	3741.0	4030.3
	$V_0=137.8058$ a.u. $B=170.90978$ kbar $\gamma=2.39004$		$V_0=122.6615$ a.u. $B=208.99432$ kbar $\gamma=2.43219$	

The existing experimental data on the EOS of Li (Refs. 46, 47, and 53–57) fall into three categories: piston data up to 45 kbar (Refs. 46 and 57, see Ref. 57 for a summary of early low-pressure EOS data), tungsten-carbide anvil data to 100 kbar,[47] and shock data to several hundred kbar.[53,54] Although the latter two sources of data are particularly useful in a high-pressure EOS study of this sort, each suffers from limitations. The tungsten-carbide anvil data are very reliable but have a rather low limit on the highest pressure attained. On the other hand, the high-pressure shock data are of questionable reliability since the 0-K isotherm must be extrapolated from the Hugoniot curve (a procedure which is not entirely straightforward[55,56]).

For Li all of the existing low-temperature EOS data derived from shock experiments are subject to criticism.[16] There is evidence[18] that the Hugoniot data taken by Bakanova *et al.*[53] are in error with the pressures being significantly too small. This in turn would inevitably lead to a corresponding error in the extrapolated 0-K isotherm. In contrast, the Hugoniot data taken by Rice[54] should be more reliable but Grover *et al.*[55] have suggested that the technique used by Rice to obtain the 0-K isotherm is unreliable and that the deduced 0-K pressures are overestimated. They reanalyzed Rice's data and obtained an EOS with much lower pressures. Unfortunately, the results obtained by Grover *et al.* are presented in a figure

TABLE VII. The EOS's for Li found in this study for the KSG and RSK models compared to previous theory and to experiment. (P in kbar and V in a.u.)

V	P^{a}	P^{b}	P^{c}	P^{d}	P^{e}
119.73	33		28.6	5.2	
118.32	35		31.4	7.9	
114.8		33	39.1	15.0	
112.34	47		45.0	20.5	
106.68	66		60.3	34.7	
103.3		62	70.9	44.6	
100.18	80		81.7	54.7	
95.85	98		98.8	70.6	
94.73	101		103.6	75.2	
91.8		109	117.3	88.0	
86.1		143	148.6	117.3	
80.4		187	187.7	154.1	
74.6		248	238.5	202.1	
131.3			8.8	−13.1	16
116.7			34.9	11.1	41
102.1			74.9	48.3	83
87.5			140.2	109.5	157
72.9			256.1	218.7	293
58.4			485.0	436.5	577
43.8			1035.4	965.8	1260

[a] Tungsten-carbide anvil, 300-K isotherm (Ref. 47).

[b] Shock data, 0-K isotherm (Ref. 54).

[c] KSG, 0-K isotherm (present).

[d] RSK, 0-K isotherm (present).

[e] Model potential, 300-K isotherm (Ref. 18).

and table (their Fig. 1 and Table I) which are mutually contradictory. In addition they do not indicate what the reference volume is for either the table or the figure. For these reasons we have been unable to make a useful comparison with their data and instead have relied on Rice's 0-K isotherm for high-pressure comparisons.

In Table VII, we compare the present EOS's with the 300-K isotherm obtained using the tungsten-carbide anvil technique,[47] the 0-K isotherm extrapolated by Rice,[54] and with the theoretical 300-K isotherm obtained by Young and Ross[18] using model potentials. (The other existing model-potential calculations[16,17] were restricted to much lower pressures and are generally consistent with Ref. 18.) Over the pressure range of 30—100 kbar, the KSG EOS for Li is in good agreement with the anvil data.[47] (Note that the experimental EOS below 69 kbar is for the bcc structure.) It is quite interesting that the 0-K isotherm deduced by Rice[54] lies slightly below the anvil data, since Grover *et al.* felt that Rice's pressures were too high. This suggests that Rice's data may in fact provide a reasonable representation of the 0-K isotherm up to the highest pressures given (about 250 kbar). In the range of pressures 100—250 kbar, the KSG EOS is again in excellent agreement with experiment (given the quality of the experimental data), while the RSK isotherm significantly underestimates the pressure. Compared to the present results and experiment, the model-potential calculation[18] gives pressures which are consistently too large.

In general, the KSG model gives a reasonable representation of the EOS for Li at least up to 250 kbar. In contrast, the more sophisticated RSK model seriously underestimates the pressures over that range.

IV. ONE-ELECTRON PROPERTIES

Although the one-electron eigenvalues obtained in density-functional theory have no rigorous physical interpretation, the band structure near the Fermi level is generally believed to correlate well with electronic excitation energies in metals. Since virtually nothing has been published about the band structure of fcc Li, at least a qualitative discussion of the one-electron properties is warranted. For this purpose the RSK model should be superior to the KSG model and discussion is restricted to the former (the qualitative features are not affected by the choice of the LDA model).

The band structure of fcc Li at low pressure ($a = 7.9375$ a.u.) is shown in Fig. 1. (For a bcc Li band structure substantially the same as ours see Ref. 10.) The band structure in Fig. 1 is in qualitative disagreement with the stereotypical picture of an alkali metal, as might be expected on grounds of space-group differences alone. The traditional picture envisions a nearly spherical Fermi surface which never makes contact with the boundaries of the BZ,[58] i.e., the surface is closed. In contrast, the present band structure for fcc Li has an open Fermi surface with narrow necks centered on the L points touching the zone boundary. In this respect fcc Li resembles the monovalent noble metals (Cu, Ag, and Au).[59]

As fcc Li is subjected to pressure, the qualitative

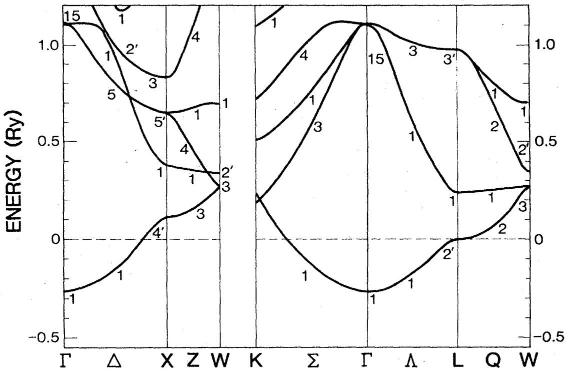

FIG. 1. Band structure of fcc Li for $P=0.0$ Mbar ($a=7.9375$ a.u.) using the Rajagopal-Singhal-Kimball (RSK) model (Ref. 40).

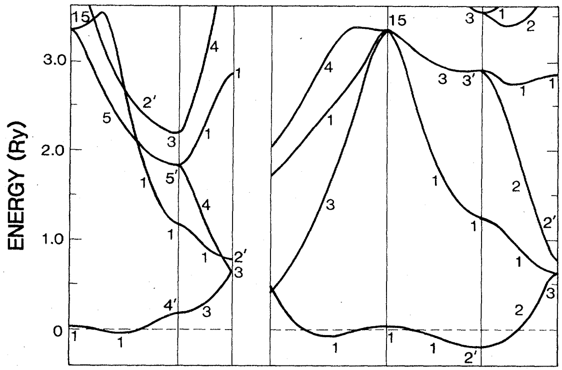

FIG. 2. Band structure of fcc Li for $P=3.7$ Mbar ($a=4.6412$ a.u.) using the Rajagopal-Singhal-Kimball (RSK) model (Ref. 40).

features of the band structure remain unaltered up to at least 700 kbar. Quantitatively, the *sp*-hybridized bands steadily broaden and the diameter of the necks in the Fermi surface increases. However, for extreme high pressures the band structure and Fermi surface become radically altered. Figure 2 shows the band structure of fcc Li at 3.7 Mbar ($a=4.6412$ a.u.). Although the bulk of the *sp*-hybridized bands are qualitatively the same as in Fig. 1, the bands are highly distorted in the region near the Fermi energy. The occupied part of the conduction bands is no longer parabolic with the minimum energy at the zone center. Instead the minimum is at the L point and a pocket of holes has formed at the center of the BZ. As a result of these changes, the occupied bandwidth is actually smaller at 3.7 Mbar than it was at 0.0 Mbar (0.193 Ry versus 0.266 Ry).

The drastic pressure induced modifications to the band structure are due to an l dependence in the broadening of the bands. Although all of the bands are broadened by pressure, the p band is broadened more rapidly than the s band and hence the bottom of the p band passes through the s band. Since the singly degenerate state at the center of the BZ is a pure s state while the lowest state at the L point is a pure p state, those two states become reversed in order. One would anticipate that the lowest-energy state at the X point might also move below the center of the band for sufficiently high pressures. These qualitative features of the band structure shown in Fig. 2 have been confirmed in a recent LMTO calculation performed at a similar compression.[60]

The band structure for fcc Li at 3.7 Mbar appears, at least superficially, to contradict the general belief that at high pressures all materials will become free-electron-like. That is, these calculations show Li to be very free-electron-like at low pressure and less so for pressures up to 3.7 Mbar. However, one must note that for sufficiently elevated pressures the $1s$ band must eventually broaden and come in contact with the bottom of the $2p$ band to form the expected free-electron-like continuum. (At 3.7 Mbar, the $1s$ band is 0.306 Ry wide and lies 3 Ry below the conduction band.) Thus the present work does not suggest that the free-electron limit is nonexistent but rather demonstrates that limit to be achievable only for pressures far beyond the capability of current experimental technique, even for the simplest of metals. Although the predictions made here are less dramatic than the recent prediction of a high-pressure insulating phase in Ni,[61] they do confirm the existence of more-complicated one-electron properties at high pressures than might have been anticipated.

V. CONCLUSIONS

Based on the present calculations, two important conclusions may be made concerning the crystallographic phase stability of Li. The first of these is that a careful LDA calculation predicts that the zero-pressure and -temperature phase of Li is indeed close packed. This result is consistent with the available (somewhat ambiguous) experimental data.

The second important result is the absence of any $T=0$-K transition to the bcc structure for cell volumes ranging from 0.175 to 3.0 times the experimental zero-pressure volume. The remarkable stability of the close-packed structure in Li up to at least 4 Mbar is consistent with existing evidence[19,32–35] that the phase stability of elemental solids is intimately related to the d occupancy near the Fermi level. Since all of the d states for Li lie well above the Fermi level, the usual sd-hybridization mechanism is not available to trigger a transition to the bcc structure. One might have anticipated that for Li the p states would perform the same function as the d states play in heavier materials. However, in light of the strong sp-hybridization effects on the band structure of Li at 3.7 Mbar, it is clear that sp hybridization is not a sufficient mechanism to induce an fcc-bcc transition.

The present values for the zero-pressure lattice constant are slightly smaller than the corresponding values obtained using muffin-tin methods. It is probable that the spherical averaging used in the muffin-tin approximation reduces the effectiveness of the bonding in Li and a similar effect is likely to occur in all those elemental solids whose binding is largely due to sp hybridization.

There are systematic differences between the results obtained using the KSG model and those obtained with the RSK model. At zero pressure, the KSG lattice constant and bulk modulus are more realistic, while the RSK binding energy is substantially closer to experiment. These results are consistent with the findings of Jansen *et al.*[41] for Fe. However, the present work also shows that the KSG model gives a better description of the P versus V curve up to at least 250 kbar. Whether these differences point to the need for a better LDA model or to nonlocal corrections is a matter of conjecture.

ACKNOWLEDGMENTS

We thank R. C. Albers for performing LMTO calculations on compressed Li, confirming our high-pressure one-electron results. We acknowledge useful conversations with A. M. Boring and J. Callaway. This work was performed in part under the auspices of the U.S. Department of Energy. This work was funded in part by the National Science Foundation under Grant No. DMR-82-18498.

---

[1] E. Wigner and F. Seitz, Phys. Rev. **43**, 804 (1933); F. Seitz, *ibid.* **47**, 400 (1935).

[2] W. Y. Ching and J. Callaway, Phys. Rev. B **9**, 5115 (1974).

[3] J. P. Perdew and S. H. Vosko, J. Phys. F **4**, 380 (1974).

[4] N. W. Ashcroft and D. C. Langreth, Phys. Rev. **155**, 682 (1967).

[5] W. E. Rudge, Phys. Rev. **181**, 1033 (1969).

[6] D. A. Liberman, Phys. Rev. B **2**, 244 (1970).

[7] F. W. Averill, Phys. Rev. B **6**, 3637 (1972).

[8] L. Kumar, H. J. Monkhorst, and F. E. Harris, Phys. Rev. B **9**, 4084 (1974).

[9] L. Kumar, and H. J. Monkhorst, J. Phys. F **4**, 1135 (1974).

[10] J. F. Janak, V. L. Moruzzi, and A. R. Williams, Phys. Rev. B **12**, 1257 (1975); V. L. Moruzzi, J. F. Janak, and A. R. Williams, *Calculated Electronic Properties of Metals* (Pergamon, New York, 1978).

[11] J. D. Pack, H. J. Monkhorst, and D. L. Freeman, Solid State Commun. **29**, 723 (1979).

[12] J. R. Chelikowski, Phys. Rev. B **21**, 3074 (1980).

[13] J. Callaway, X. Zou, and D. Bagayoko, Phys. Lett. **89A**, 86 (1982).

[14] J. Callaway, X. Zou, and D. Bagayoko, Phys. Rev. B **27**, 631 (1983).

[15] J. A. Moriarty, Phys. Rev. B **26**, 1754 (1982).

[16] V. G. Vaks, S. P. Kravchuk, and A. V. Trefilov, Fiz. Tverd. Tela (Leningrad) **19**, 1271 (1977) [Sov. Phys.—Solid State **19**, 740 (1977)], and references therein.

[17] T. Soma, J. Phys. F **10**, 1401 (1980).

[18] D. A. Young and M. Ross, Phys. Rev. B **29**, 682 (1984); M. Ross, *ibid.* **21**, 3140 (1980).

[19] H. L. Skriver, Phys. Rev. B **31**, 1909 (1985).

[20] R. W. Shaw, as quoted by V. Heine and D. Weaire, in *Solid State Physics*, edited by H. Ehrenreich, F. Seitz, and D. Turnbull (Academic, New York, 1970), Vol. 24.

[21] R. Pick, as quoted by V. Heine and D. Weaire, in *Solid State Physics*, edited by H. Ehrenreich, F. Seitz, and D. Turnbull (Academic, New York, 1970), Vol. 24.

[22] J. Donohue, *The Structures of the Elements* (Wiley, New York, 1974), and references therein; J. P. Day and A. L. Ruoff, Phys. Status Solidi A **25**, 205 (1974).

[23] See, for example, K. Asaumi, Phys. Rev. B **29**, 7026 (1984).

[24] P. Hohenberg and W. Kohn, Phys. Rev. **136**, B864 (1964).

[25] W. Kohn and L. J. Sham, Phys. Rev. **140**, A1133 (1965); see also, R. Gaspar, Acta Phys. Hung. **3**, 263 (1954).

[26] J. C. Boettger and S. B. Trickey, Phys. Rev. B **29**, 6425 (1984).

[27] M. Ross and A. K. McMahan, Phys. Rev. B **21**, 1658 (1980).

[28] A. K. Ray, S. B. Trickey, R. S. Weidman, and A. B. Kunz, Phys. Rev. Lett. **45**, 933 (1980).

[29] J. C. Boettger and S. B. Trickey, Phys. Rev. B **29**, 6434 (1984).

[30] M. T. Yin and M. L. Cohen, Phys. Rev. B **24**, 6121 (1981).

[31] M. T. Yin and M. L. Cohen, Phys. Rev. Lett. **45**, 1004 (1980).

[32] P. K. Lam and M. L. Cohen, Phys. Rev. B **27**, 5986 (1983).

[33] J. A. Moriarty, Phys. Rev. B **8**, 1338 (1973).

[34] H. L. Skriver, Phys. Rev. Lett. **49**, 1768 (1982).

[35] A. K. McMahan and J. A. Moriarty, Phys. Rev. B **27**, 3235 (1983).

[36] J. W. Mintmire, J. R. Sabin, and S. B. Trickey, Phys. Rev. B **26**, 1743 (1982).

[37] J. C. Boettger and S. B. Trickey (unpublished).

[38] See, for example, H. L. Skriver, *The LMTO Method* (Springer, Berlin, 1984).

[39] U. von Barth and L. Hedin, J. Phys. C **5**, 1629 (1972).

[40] A. K. Rajagopal, Adv. Chem. Phys. **41**, 59 (1979).

[41] H. J. F. Jansen, K. B. Hathaway, and A. J. Freeman, Phys. Rev. B **30**, 6177 (1984).

[42] C. S. Wang and J. Callaway, Comput. Phys. Commun. **14**, 327 (1978).

[43] J. C. Boettger and S. B. Trickey, Comput. Phys. Commun. **32**, 361 (1984).

[44] F. W. Averill and G. S. Painter, Phys. Rev. B **24**, 6795 (1981).

[45] J. C. Boettger and S. B. Trickey (unpublished); see also Ref. 29.

[46] M. S. Anderson and C. A. Swenson, Phys. Rev. B **31**, 668 (1985).

[47] B. Olinger and J. W. Shaner, Science **219**, 1071 (1983).

[48] See, for example, N. F. Mott, Philos. Mag. B **50**, 161 (1984).

[49] F. D. Murnaghan, Proc. Natl. Acad. Sci. USA **30**, 244 (1944); O. L. Anderson, J. Phys. Chem. Solids **27**, 547 (1966).

[50] K. A. Gshneider, Solid State Phys. **16**, 276 (1964).

[51] L. Hedin and B. I. Lundqvist, J. Phys. C. **4**, 2064 (1971).

[52] A. R. Mackintosh and O. K. Andersen, in *Electrons at the Fermi Surface*, edited by M. Springford (Cambridge University, Cambridge, New York, 1980); O. K. Andersen, H. L. Skriver, H. Nobl, and B. Johansson, Pure Appl. Chem. **52**, 93 (1979).

[53] A. A. Bakanova, I. P. Dudoladov, and R. F. Trunin, Fiz. Tverd. Tela **7**, 1615 (1965) [Sov. Phys.—Solid State **7**, 1307 (1965)].

[54] M. H. Rice, J. Phys. Chem. Solids **26**, 483 (1965).

[55] R. Grover, R. N. Keeler, F. J. Rogers, and G. C. Kennedy, J. Phys. Chem. Solids **30**, 2091 (1969).

[56] R. Grover, J. Phys. Chem. Solids **32**, 2539 (1971).

[57] S. N. Vaidya, I. C. Getting, and G. C. Kennedy, J. Phys. Chem. Solids **32**, 2545 (1971).

[58] N. W. Ashcroft and N. D. Mermin, *Solid State Physics* (Holt, Rinehart, and Winston, New York, 1976), pp. 284—288.

[59] N. W. Ashcroft and N. D. Mermin, in Ref. 58, pp. 288—293.

[60] R. C. Albers (unpublished).

[61] A. K. McMahan and R. C. Albers, Phys. Rev. Lett. **49**, 1198 (1982).